

# Design of a polarized head-mounted projection display using FLCOS microdisplays

Rui Zhang, Hong Hua<sup>\*</sup>

College of Optical Sciences, The University of Arizona, Tucson, AZ, 85721

## ABSTRACT

Head-mounted projection display (HMPD) technology, as an alternative to conventional head mounted displays (HMD), offers the potential of designing wide field-of-view (FOV) optical see-through HMDs. Due to multiple passes through a beamsplitter, however, existing HMPD designs suffer from low luminance efficiency and thus the displayed image is lack of brightness and contrast. The design of a polarized head-mounted projection display (p-HMPD) was recently proposed. The major departure of a p-HMPD design from other existing HMPD systems is the usage of polarization management to minimize light loss through beamsplitting. A p-HMPD consists of a pair of projections lenses, microdisplays, polarization control elements, and retroreflective sheeting material as a projection screen. In this paper, we explore the usage of a ferroelectric liquid-crystal-on-silicon (FLCOS) microdisplay as the image source and present a compact design of an illumination unit with double telecentric optics to achieve highly bright and uniform illumination on the FLCOS microdisplay. The key contribution of this design lies in the compactness which is a critical factor in HMD systems. The first-order optics and the transformation of polarization in the design will be described in detail. The simulation of the illumination unit will be shown and its luminous efficiency and uniformity will be discussed. Based on this illumination engine, we will further describe the design of a compact projection lens and discuss the overall performance of the optics.

**Key words:** Head-mounted projection display, head-mounted display, light engine, projection lens

## 1. INTRODUCTION

Mixed- and augmented reality (MR-AR) technology seeks to selectively supplement, rather than replace, a user's sensory perceptions of the physical world with computer-generated digital information. A wide range of applications have been explored and examples include surgical planning, medical training or engineering design.<sup>1</sup> Among the display technologies used for MR-AR systems, optical see-through head-mounted displays (HMD) are one of the basic approaches to optically combining computer-generated images with real-world scenes through an optical combiner interface such as a beamsplitter. The optical see-through approach allows a user to see the real world with full resolution and thus is preferred for tasks where hand-eye coordination or non-blocked real-world view is critical.

Designing a wide field-of-view (FOV), compact and non-intrusive optical see-through HMDs, however, has been challenging. Head mounted projection display (HMPD) technology, pioneered by Fisher,<sup>2</sup> Kijima and Ojika,<sup>3</sup> and Fergason,<sup>4</sup> has recently been explored extensively as an alternative approach to conventional optical see-through HMD designs.<sup>5,6,7</sup> It is considered as a technology lying on the boundary between conventional HMDs and CAVE-like projection displays.<sup>8</sup> Two major aspects distinguish the HMPD technology from conventional HMDs and projection systems: projection optics are used to replace eyepiece- or microscope-type lenses in a typical HMD design and retro-reflective screens are used to substitute a typical diffusing screen in a conventional projection system. The unique combination of projection and retro-reflection not only enables stereoscopic capability, but also provides intrinsically correct occlusion of computer-generated object by the real object and offers the capability of designing wide FOV optical see-through HMDs.<sup>5</sup> Several efforts have been made to custom-design compact projection optics and display prototypes.<sup>6, 7, 9, 10</sup>

---

<sup>\*</sup> Email: [hhua@optics.arizona.edu](mailto:hhua@optics.arizona.edu); phone: 1 520 626 8703; web: [3dvis.optics.arizona.edu](http://3dvis.optics.arizona.edu)

It has been a common problem in optical see-through HMDs that the displayed image is lack of image brightness and contrast compared to the direct view of a real-world scene. This is mainly due to the light attenuation through a beamsplitter interface and the lack of ultra-bright microdisplays. For instance, using a 50/50 beamsplitter, the displayed image is at most half of the microdisplay luminance. This problem becomes aggravated in HMPDs in which light is split twice by a beamsplitter, and thus theoretically at least 75% of image luminance is attenuated and the actual luminance efficiency is even lower due to the loss through an imperfect retro-reflective screen. By roughly estimating, the actual luminance efficiency of existing HMPD designs is around 4~10% or less of the image source luminance. For instance, assuming the usage of a miniature backlit active matrix liquid crystal display (AMLCD) as the image source, the peak luminance of such microdisplay is typically around  $100 \text{ cd/m}^2$  and, with only 4% of light efficiency, the luminance of the observed image is about  $4 \text{ cd/m}^2$ , while the average luminance of a well-lit indoor environment is about  $120 \text{ cd/m}^2$ . As a result, the low-brightness image of HMPDs will appear washed out in such well-lit environments. In fact, most optical see-through HMDs, including HMPDs, are typically operated under a dimmed lighting condition.

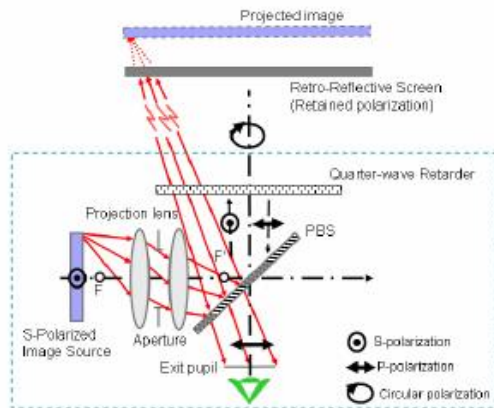


Fig. 1. Schematic design of a p-HMPD

is reflected by the PBS, it is retro-reflected back to the same PBS by a retro-reflective screen. The depolarization effect by the retro-reflective screen was recently tested with an Axometric® polarimeter, which is less than 10% within  $\pm 20$  degrees and is less than 20% up to  $\pm 30$  degrees. As a result, the retro-reflected light remains dominantly the same polarization as its incidence light. In order to achieve high transmission through the PBS after the light is retro-reflected back, a quarter-wave retarder is placed between the PBS and the retro-reflective screen. The fast axis of the quarter-wave retarder is set to be at 45 degrees with the polarization direction of the s-polarized light, thus it converts the s-polarized light into circular polarized light after the first pass and converts the retro-reflected circular polarized light into a p-polarized light after the second pass through the retarder. Consequently, the light is converted from the state of high-reflection polarization to the high-transmission polarization and is sent back to the exit pupil where the eye is so that the projected image can be observed. By assuming zero absorption and perfect polarization management, the luminance transfer efficiency in the p-HMPD design is theoretically three times higher than that of non-polarizing HMPD designs using a theoretical 50/50 beamsplitter. Practically, we expect the observed image luminance will be averagely about two times brighter if all other optical components are identical.

Another way to improve the luminance output of HMPDs is to use brighter microdisplays with higher luminance. In this paper, we will present the development of a bright p-HMPD prototype using ferroelectric Liquid-crystal-on-Silicon (FLCOS) microdisplays as the image sources. The FLCOS microdisplays operate in reflective mode, opposed to the transmission mode of backlit AMLCDs, thus has higher luminous efficiency.

## 2. SYSTEM DESIGN

In our current HMPD prototypes, 1.3'' color AMLCDs were used as the image sources and these microdisplays have a resolution of  $(640 \times 3) \times 480$  pixels and use 1.4'' Alphalight RGB LED panels by Teledyne Inc. as the backlighting sources. When designing a new p-HMPD prototype, with the rapid development of display technology, we attempt to explore available microdisplay technologies that offer higher resolution, more compact packaging, and higher luminance output.

To address this problem, the design of a polarized head-mounted projection display (p-HMPD) was proposed,<sup>11</sup> in which the polarization states of the light are carefully manipulated to achieve high light efficiency. A schematic illustration of a monocular p-HMPD configuration is shown in Fig. 1. One of the modifications is to replace a non-polarizing beamsplitter in conventional HMPD systems with a polarizing beamsplitter (PBS). A PBS splits non-polarized incident light into s-polarized and p-polarized light in the paths of reflection and transmission, respectively. The image on the microdisplay is projected through a projection lens to form a magnified image. To gain maximum reflection and minimize the transmission loss of light incident upon the PBS from the projection optics, the light from the image source is manipulated to be s-polarized so that its polarization direction is matched with the high-reflection polarization of the PBS. After the projected light

Table 1 summarizes the major properties of several candidate microdisplay technologies, including AMLCD, organic light emitting displays (OLEDs), liquid crystal on silicon (LCOS) and FLCOS. It is worth noting that most of these data were adopted from the websites of the display manufacturers.

Table 1 Properties of Microdisplay for HMDs

|                                 | Active matrix LCD | OLED           | LCOS                                 | FLCOS                                     |
|---------------------------------|-------------------|----------------|--------------------------------------|---|
| Manufacturer                    | Kopin®            | Emagin®        | Brilliant®                           | Forth dimension®                          |
| Size(diagonal) (inch)           | 0.97              | 0.61           | 0.75~0.86                            | 0.88                                      |
| Resolution (pixel)<br>(Maximum) | 1280x1024         | 800x600        | 1600x1200                            | 1280x1024                                 |
| Contrast Ratio                  | 100:1             | 100:1          | 2000:1                               | 200:1                                     |
| Pixel size (μm)                 | 15 x 15           | 15 x 15        | 9.5 x 9.5                            | 13.4 x 13.4                               |
| switching speed (ms)            | <30               | <1             | 11                                   | 0.04                                      |
| Frequency (Hz)                  | 60                | Up to 85       | Up to 120                            | 60  |
| Color method                    | RGB sub-pixels    | RGB sub-pixels | Three R-G-B panels                   | Color sequential                          |
| Color depth (bit)               | 24                | 24             | N/A                                  | 24  |
| Illumination mode               | Transmissive      | Self-emissive  | Reflective                           | Reflective                                |
| Luminance (cd/m <sup>2</sup> )  | ~100              | 70-200         | >1000 depends on<br>the light engine | Up to 1000 depends<br>on the light engine |
| Optical efficiency              | <15%              | N/A            | 70%                                  | 60-70%                                    |

Compared with FLCOS and LCOS displays, AMLCD offers a potentially more compact system because its transmissive nature only needs a backlit panel rather than a complex illumination unit. However, it has relatively low contrast ratio and provides the lowest luminance range and largest pixel dimensions among all of the above technologies. The self-emission nature of the OLED and its compact packaging offer potentially the most compact system design among these technologies, and it provides a good range of luminance. However, the resolution and contrast ratio of existing OLEDs are relatively low compared with FLCOS and LCOS microdisplays, and its life span would be shortened if the display luminance is high (e.g. more than 100 cd/m<sup>2</sup>). Another disadvantage is its relatively small panel size. For HMD designs, a display panel around one inch is preferred as it offers a good balance of compactness and the focal length range of the optics. When the display panel is too small, it requires a shorter focal length and larger magnification to achieve a reasonable FOV, which leads to a challenging design of a low F/# system. Currently LCOS microdisplays offer the highest resolution and contrast compared with other types of displays and they are commonly used as image sources in digital projectors. The liquid crystal used in LCOS microdisplays, however, has low switching speed, which makes it impossible to use color sequential method, like FLCOS displays, to achieve full color mode. Generally more than two display panels and a bulky illumination system are needed in a full-color system. FLCOS offers high pixel resolution, luminance output, image contrast, and optical efficiency. The fast response speed of ferroelectric liquid crystal makes it possible to achieve full-color display using a single-panel color sequential scheme. On the other hand, it requires a carefully designed illumination unit to achieve high contrast and high luminance, which makes the overall display system less compact than a system using AMLCD or OLED microdisplays.

Taking into account the pros and cons of the various technologies discussed above, we choose to use the SXGA-R2D FLCOS microdisplay kit by *Forth Dimensional Displays Limited* (<http://www.forthdd.com>). The usage of FLCOS microdisplays makes the prototype design of a p-HMPD quite different from the previous designs of HMPD optics<sup>9,10</sup>. Table 2 lists the major differences between a p-HMPD and a non-polarizing HMPD system using AMLCDs.

One of the key differences is the requirement for illumination units. The reflective FLCOS microdisplay requires a custom-designed front illumination system to illuminate the microdisplay. In this paper the illumination unit for the microdisplay is called light engine which is a term commonly used in the projector industry. The FLCOS display is considered as the combination of a mirror and an electrically switchable quarter-wave retarder formed by the liquid crystal layer.<sup>12</sup> The retardance of the microdisplay is a function of the optical path length of rays through liquid crystal material. The FLCOS microdisplay works most efficiently when the illumination rays are normally incident upon the display surface. In normal incidence, all the rays experience the same optical path through the liquid crystal material, while skewed incidence leads to reduction of image contrast. To ensure the high contrast of the output image, it is recommended to limit the incident angle to the range of  $\pm 16$  degrees, which imposes a critical requirement on the design of both a light engine and projection lens. One of the key requirements for the illumination engine is image-space

telecentric so that for every pixel on the display surface the incident chief ray is normal to the display surface, the incident ray bundle is symmetric and the cone angle is smaller than 16 degrees.

Owing to the reflective nature of the microdisplays, the telecentric ray bundles incident upon the display surface will be mirror-reflected by the microdisplay. Thus the output ray bundles from every pixel of the microdisplay will be telecentric with a cone angle smaller than 16 degrees. To efficiently collect rays from the microdisplay and form a projected image with uniform illumination, it is required that the projection lens be image-space telecentric. On the contrary, a projection system using backlit AMLCDs, which has a relatively large viewing angle and thus relaxed requirement for the angle of incidence ray bundles, can relax the telecentric constraint to gain compactness.<sup>9</sup>

Table 2. Comparison between HMPD and p-HMPD system

|                   | HMPD                | p-HMPD                  |
|-------------------|---------------------|-------------------------|
| Microdisplay      | AMLCD               | FLCOS                   |
| Illumination mode | Transmissive        | Reflective              |
| Illumination unit | LED panel           | Light engine            |
| Luminance         | ~4cd/m <sup>2</sup> | >100cd/m <sup>2</sup>   |
| Resolution        | 640 x 480           | 1280 x 1024             |
| Polarization      | Non-polarizing      | Polarizing              |
| Projection lens   | Non-telecentric     | Image-space telecentric |
| Pixel size        | 42μm x 42μm         | 13.6μm x 13.6μm         |

### 3. DESIGN OF A LIGHT ENGINE FOR FLCOS MICRODISPLAYS

FLCOS microdisplay, which operates in reflection mode and can be thought as a reflective light modulator, offers bright and uniform illumination only in telecentric mode. In this section, we present a compact design of a light engine to achieve bright and uniform illumination for FLCOS microdisplays.

#### 3.1 Source selection

There are many available sources, such as tungsten filament lamps and LED sources. For HMPD application, there are several constraints on the source selection and the light engine design. First, safety is a primary concern in any head-mounted devices. Therefore sources with low power consumption and low heat dissipation are highly desired. Secondly, compactness and lightweight are always critical for HMD systems. Finally, in order to generate an image with high brightness and uniformity across the whole FOV, the illumination on the microdisplay should be uniform and bright.

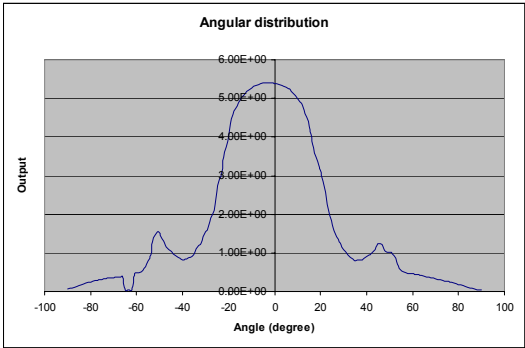


Fig. 2. Angular distribution of LED illuminator

Table 3. Specification of microdisplay and LED illuminator

| Parameters         | Specifications         | Parameters        | Specification  |
|--------------------|------------------------|-------------------|--|
| FLCOS microdisplay |                        | LED panel         |  |
| Size               | 22.3mm                 | Body Dimensions   | 18.4 x 14.1mm  |
| Active area        | 17.43 x 13.95 mm       | Active area       | 8.4 x 6.5mm  |
| Resolution         | 1280x 1024 pixels      | Weight            | 4 ± .5 grams   |
| Pix size           | 13.6 μm                | Luminance         | 34800 (cd/m <sup>2</sup> )   |
| Color technique    | Field sequential color | Color Coordinates | Red: x = .67-.43, y = .27-.33<br>Green: x=.14-.28, y = .64-.73<br>Blue: x = .11-.15, y = .04-.10 |
|                    |                        | Power             | 340mW  |

A 0.5" Alphalight® color LED illuminator by Teledyne Inc. is selected for our p-HMPD prototype design. The illuminator is compatibly driven by the color sequential technique of the FLCOS displays. Table 3 summarizes the major specifications of the microdisplay and illuminator. This LED illuminator has advantages of low power consumption, small size, and high luminance. Fig. 2 shows the intensity distribution of the LED panel and its full width at half maximum (FWHM) is 23 degrees.<sup>13</sup>

### 3.2 Schematic design of light engine

The design of illumination systems for reflective LCDs has been well explored in digital projector industry and perhaps one of the most popular light engine designs is the usage of a paired fly's eye lens array system combining with condenser lenses to achieve uniform illumination with high efficiency on the microdisplays<sup>14</sup>. However, this design usually requires a long optical path, i.e. 120mm at least, and is too bulky to be used for head-mounted applications.

As discussed in Section 2, one of the key requirements for the illumination engine is image-space telecentric. Furthermore, as shown by the luminous distribution property of the LED illuminator in Fig. 2, the emitted ray intensity decreases as the ray angle with the normal of illuminator surface increases. The rays within the cone angle of 23 degrees carry about 38.6% of the total energy. With these considerations, we present a novel compact design of a light engine using the concept of Abbe illumination in which a light source is imaged directly on the microdisplay.

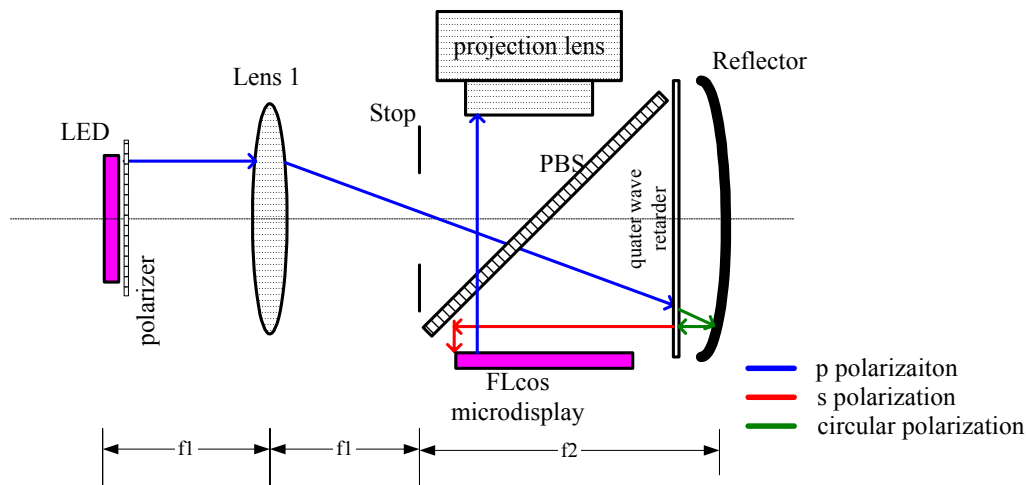


Fig. 3. Design of a light engine for FLCOS microdisplays

Fig. 3 illustrates the schematic design of the proposed light engine. This design, in addition to being an Abbe illumination system, is a double telecentric system in which the chief ray (i.e. the ray passing through the center of the stop) is parallel to the axis of the system in both of the object and image spaces. The double telecentric is achieved by placing the stop at the common focal point of lens 1 and the reflector. Different from an ordinary double telecentric system composed by the condenser lenses, in our system, an aspheric Fresnel lens is used for the lens 1 because of its feasibility of low  $f/\#$  and light weight.<sup>15</sup> The groove side of the Fresnel lens is set to face the LED to achieve high light efficiency.<sup>16</sup> The Reflector, which is free of spherical and chromatic aberrations, is used as second optical element to fold the optical path for the purpose of a more compact solution.

Polarization elements are used in the design to increase light efficiency and achieve high contrast. A linear polarizer filters the non-polarized light emitted by the LED panel into p-polarized source, which transmits maximally through a PBS placed in front of the reflector. A quarter-wave retarder is placed between the PBS and the reflector and its fast axis is set to be at 45 degrees with the direction of p-polarized light. By passing twice through the retarder, the transmitted p-polarized light is then converted into s-polarized light after the reflection by the reflector and is maximally reflected by the PBS onto the microdisplay. The output light of the FLCOS microdisplay which is equivalent to the combination of a mirror and a quarter-wave retarder is p-polarized and will maximally transmit through the PBS and be collected by the projection lens.

Table 4 shows the first order data of the design. The LED placed at the front focal point of the lens 1 forms an image on the FLCOS microdisplay which is placed at the conjugate position to the focal point of reflector through a PBS. The ratio of the reflector focal length ( $f_2$ ) to the focal length ( $f_1$ ) of the lens 1 is the same as the ratio of microdisplay size to that of the LED panel. The stop is used to limit the cone of light beam from each point on the LED, and it helps to make a uniform illumination on microdisplay. In our design, the stop size is set to allow rays within the cone angle of  $\pm 23$  degrees to pass through system. Within this cone angle, roughly 38.6% of total energy will pass through the system. Considering the loss through a linear polarizer, theoretically 19.3% of total energy will be collected by the illumination optics and illuminates the microdisplay. Increasing the stop size and thus the cone angle can collect more rays, but it compromises overall system compactness. In this double-telecentric design, the rays emitted normally from the LED panel surface, which have the highest luminance, are incident upon the microdisplay at a normal angle, yielding most efficient reflection.

Table 4 First-order data of the light design

|              | Lens 1 | Reflector |               | PBS     | Retarder      | Polarizer |
|--------------|--------|-----------|---------------|---------|---------------|-----------|
| Focal length | 15mm   | 35mm      | Size(mm)      | 37 x 30 | 40 (Diameter) | 8.4 x 6.5 |
| Diameter     | 25mm   | 35mm      | Thickness(mm) | 1.6     | 0.5           | 0.5       |
| f/#          | 0.6    | 1         |               |         |               |           |

The optical magnification of the Abbe illumination system is given as

$$m = h'/h = f_2/f_1 \quad (1)$$

where  $h$  and  $h'$  are the size of the LED panel and microdisplay, respectively. Considering the aspect ratio difference of the LED panel and microdisplays, the magnification in our design was set to be 2.3. The maximum ray angle incidence upon the microdisplay is calculated through the equation:

$$X = uh = u'h' \quad (2)$$

where  $u = \tan(\theta)$ , and  $u' = \tan(\theta')$ . Here  $\theta$  is marginal ray angle in the object space, and  $\theta'$  is the marginal ray angle in the image space. As the stop size constrains the angle  $\theta$  to be 23 degrees, through the equations (1) and (2), the angle  $\theta'$  turns to be 10.5 degrees which is smaller than 16 degrees.

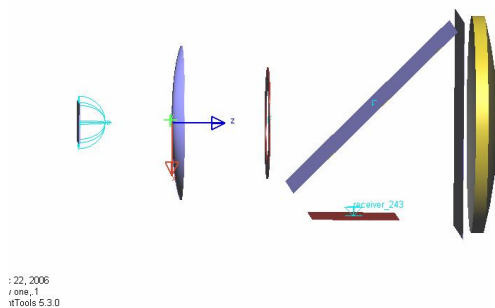


Fig. 4. Simulated model of the light engine

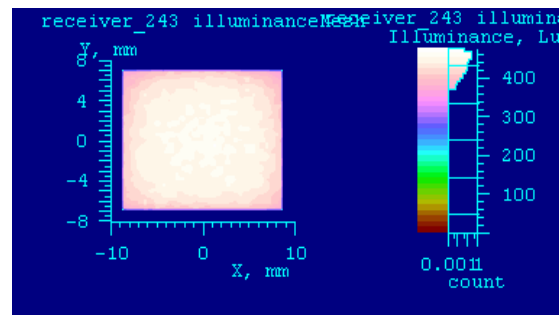


Fig. 5. Illuminance distribution on the microdisplay

### 3.3 Simulation of the light engine

In order to better examine the light efficiency and illumination uniformity, the light engine design described in the previous sub-section was modeled using LightTools®<sup>17</sup> (Fig. 4). The emission profile of the LED panel was modeled using its angular intensity distribution data (Fig. 2), and the total power of the source was set to be 1 lumen. All the other components were modeled according to their optical properties and geometrical measurements of the real parts. A receiver was placed on the microdisplay to estimate the efficiency of the light engine and to evaluate the light distribution on the microdisplay. Fig. 5 shows the output illuminance distribution on the microdisplay by tracing about 50 million rays through the system. The standard deviation of the illuminance distribution across the display area is about 4.5% and the maximum illuminance difference is about 23.8%. The total flux on the microdisplay is 0.11 lumens, which suggests that about 11% of the total energy emitted by the LED is collected by the microdisplay. This efficiency is considered to be reasonably close to the theoretical prediction of 19.3% in the previous sub-section. The overall efficiency can be further improved with a compromise of a less compact design.



## 4. DESIGN OF PROJECTION LENS

The use of FLCOS microdisplay requires a projection system with the constraint of image-space telecentric, which makes designing a high performance, compact, lightweight system very challenging. In this section, we will describe the design process of a compact projection system and discuss the performance and problem of a preliminary design.

### 4.1 Overall specification

Although projection optics does not scale as much with the increase of FOV as eyepiece-type optics, which makes designing wide FOV, optical see-through HMPD systems relatively easier than conventional HMDs, there are a few factors in HMPD systems that impose limits on the FOV. First of all, the use of a planar PBS or a regular beamsplitter in front of the eye (Fig.1), which is oriented at 45 degrees with the optical axis, sets up the FOV upper limit of 90 degrees. Furthermore, a wide FOV requires a large size of PBS and retarder and consequently challenges the compactness and lightweight of the display system. The limit of allowable PBS and retarder dimensions is set by the interpupillary distance (IPD), which is in the range of 55 to 75mm for over 95% of the population. Thirdly, previous investigation on retroreflective materials shows that the retro-reflectance of currently available materials drops off significantly for light incident at angles beyond  $\pm 35^\circ$ .<sup>18</sup> A FOV beyond 70 degrees will inevitably cause vignetting-like effect and compromise image uniformity. Finally, the angular resolution of the display degrades with the increase of the FOV. Taking into account these factors, we decide to aim for a projection system with a FOV of 56 degrees, which corresponds to an

effective focal length (EFL) of 21.1mm for the selected FLCOS microdisplays.

| Parameter              | Specification           |
|------------------------|-------------------------|
| Projection lens        |                         |
| Effective focal length | 21.1 mm                 |
| Entrance pupil         | 10 mm                   |
| Eye relief             | 21 mm                   |
| Image mode             | Image space telecentric |
| BFL                    | 30 mm                   |
| FOV                    | 56°                     |
| Wavelength range       | 486—656 nm              |
| Distortion             | <4% over FOV            |

In addition to being image space telecentric, the projection lens requires a large back focal length (BFL) to ensure enough space for the PBS which is placed between microdisplay and projection lens in Fig. 3. Based on the light engine design in Section 3, the BFL is chosen to be at least 30mm.

Since a user's eye is positioned at the conjugate position to the entrance pupil of the projection lens (Fig. 1), the entrance pupil diameter is very critical for comfortable observation. Typically it is suggested the pupil diameter of the projection system for HMPDs should be at least 10-12mm. This range of pupil size

allows an eye swivel of about  $\pm 21^\circ$  up to  $26.5^\circ$  within the eye sockets without causing vignetting or loss of image with a typical 3-mm eye pupil in the lighting conditions provided by HMPDs. Furthermore, it allows a  $\pm 5$ mm to 6mm IPD tolerance for different users without the need to mechanically adjust the IPD of the binocular optics. Considering the short focal length of the optics, we target for an entrance pupil with a diameter of at least 10mm, which leads to a projection system with an F/# of 2.1.

In designing a head-mounted system, an effective eye clearance of at least 20mm is necessary to accommodate users with eyeglasses. Although it is generally less challenging to achieve large eye clearance in HMPD designs than in conventional eyepiece-type HMDs, the requirement for large eye clearance can be problematic in systems with wide FOV as the dimensions of the PBS and retarders in Fig. 1 increase with eye clearance distances. Therefore, we decide a minimal 21mm eye clearance distance. The first-order specification of the projection system is summarized in Table 5.

### 4.2 Design process

#### 4.2.1 Starting lens

We start the design from a patent lens by Norihiro Nanba<sup>19</sup>. Fig 6 shows the layout of

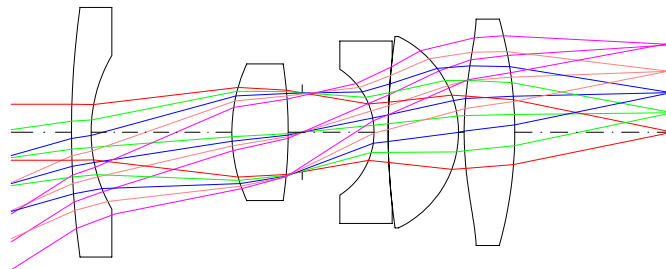


Fig. 6 Layout of the starting patent lens

the design. This patent lens is designed for a digital projector, and it is inverse-telephoto and telecentric. Unlike the double Gauss lens, the lens system has an asymmetric structure relative to the stop because of the telecentric requirement in the image space. This five-element system offers a full FOV of 65 degrees with an F/# of 2.5. Among the five elements, a doublet is used and the front surface of the last element is aspheric to help correct spherical aberration. The ratio of the BFL to the EFL of the lens is 1.13 and the ratio of the overall length (OAL) of the optics to the EFL is 3.15. The ratio of the exit pupil distance to the EFL is 13.6, which makes the system telecentric in the image space. By scaling and several cycles of optimization with CODE V®<sup>17</sup>, we obtained a lens system with 21.1mm EFL, 30mm BFL and 66mm OAL, as shown in Fig 7(a). The full FOV is set to be 56 degrees. As shown in Fig. 7b, the MTF of the lens is around 30% at the spatial frequency of 37-lp/mm, which shows acceptable performance as a starting point for the design.

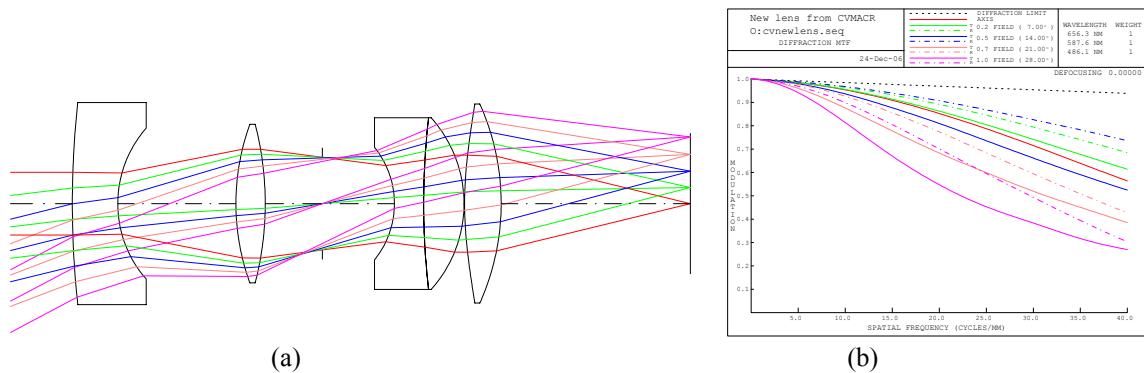


Fig. 7 Starting lens: (a) Layout; (b) MTF performance.

#### 4.2.2 Optimization

The system is rotationally symmetrical and thus the optimization is only necessary over half of the full FOV for the radial direction. Three representative wavelengths (i.e. 486nm, 589nm and 656nm) are set with the weights of 1, 2 and 1, respectively. Five fields, corresponding to 0, 7°, 14°, 21° and 28°, respectively, are used in the optimization process to represent the half FOV. The weights of the five fields were adjusted in the optimization process to balance the MTF performances across the entire FOV. During the optimization, all the surface curvatures, the surface thickness and the coefficients of aspheric surfaces were set to be variables. Several constraints were set to satisfy the specifications of the overall system and each individual lens, including the EFL, BFL, OAL, distortion requirements, and the center thickness of individual elements. The telecentric requirement was satisfied by setting the exit pupil distance to be at least 210mm from the image plane. This distance corresponds to a deviation of the chief ray by 3° from a perfectly telecentric system, which yields a good balance between the overall optical performance and the system compactness considering the difficulty in designing a perfectly telecentric lens with a short OAL.

#### 4.2.3 A compact five-element design

One of the major problems of the lens in Fig. 7a is its compactness: the OAL is too large for a head-mounted system and a more compact solution is needed. This initial system was gradually optimized by adjusting the parameter constraints and field weights through a local optimization approach. While the OAL was reduced down to about 40mm in the process of optimization, the overall performance was degraded as well. In order to further improve its performance, we set the back surface of the first lens to be aspheric, which helped to correct most of the spherical aberration. After gradual optimization, we obtained a system with satisfying performance. The lens layout and performance analysis are shown in Fig.8(a).



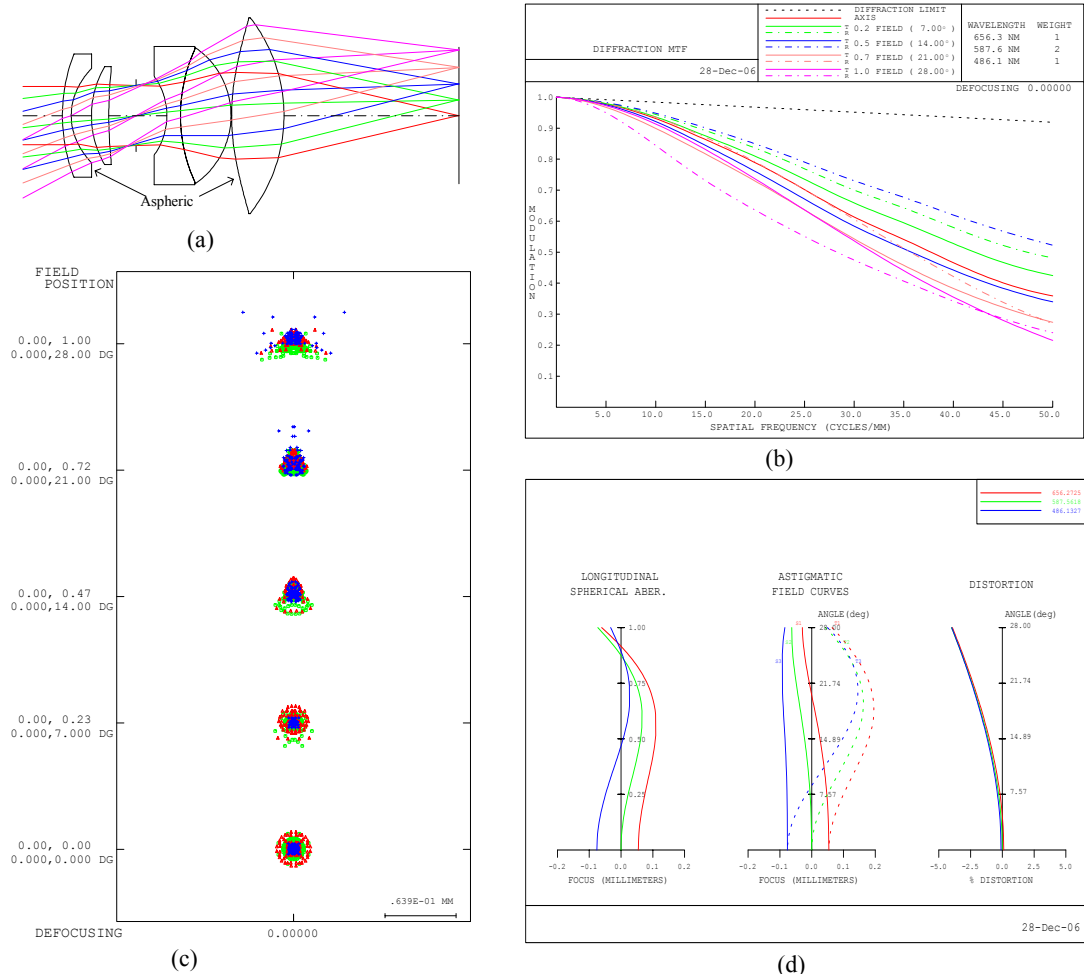


Fig. 8. Lens performance of the optimized five-element lens (a) layout of the lens (b) MTF performance (c) spot diagram (d) longitudinal spherical aberration, astigmatism and distortion.

The optical performance of the optimized lens is assessed on the image plane at the five representative field angles for three different wavelengths. MTF of the lens is presented in the Fig 8(b). The FLCOS display has a threshold spatial frequency of 36.8-lp/mm given a 13.6 $\mu$ m pixel size (i.e. threshold spatial frequency =  $1/(2 \times \text{pixel size})$ ). The modulation is about 40% at 36.8-lp/mm across the whole FOV, which means the performance of the system is currently limited by the display resolution. The spot diagrams are shown in Fig 8(c). The average RMS spot diameter across the FOV is around 16 $\mu$ m, which is slightly larger than the 13.6 $\mu$ m pixel size to avoid pixellated artifacts. Fig 8(d) shows longitudinal spherical aberration, astigmatism, and the distortion curves. The longitudinal spherical aberration and astigmatism are well balanced, and the distortion of the system is limited within 4% across the FOV.

Although this five-element lens has decent optical performance, further optimization is needed to reduce the weight of the lens. Compared with the 8-gram weight of the projection lens in our current HMPD prototypes, the five-element lens with over 35 grams weight is too heavy for head-mounted devices. From the layout of the lens shown in Fig.8(a), the doublet and the last element contribute the weight of the projection lens most. To reduce the weight, we plan to use a plastic lens with a DOE on its surface to replace the doublet and another plastic lens to replace the last element. With a DOE, we expect that most of chromatic aberration could be corrected. We aim to design a high performance lens with a total weight less than 15 grams.

## 5. CONCLUSION AND FUTURE WORK

We have presented a compact design of a p-HMPD prototype using FLCOS microdisplays. We detailed the process of designing the key parts involved in developing a prototype system, including the design of a light engine to illuminate the microdisplays and the design of a projection lens. In the future, we will further optimize the projection lens design by applying advanced optical design techniques such as diffractive optical elements and plastic materials to achieve a compact, lightweight, and high performance system. Moreover, experiments will be carried out to characterize polarization properties of each element, quantify the flux efficiency of the overall system, and examine depolarization effect. Finally, we will design a helmet system and develop a head-mounted prototype.

## ACKNOWLEDGEMENT

The paper is based on work supported by National Science Foundation (NSF) grants IIS 05-34777 and 04-11578.

## REFERENCES

1. R. Azuma, A Survey of Augmented Reality in *Presence: Teleoperators and Virtual Environments* 6, 4, 355-385, (1997).
2. R. Fisher, "Head-mounted projection display system featuring beam splitter and method of making same," US Patent 5,572,229, (1996)
3. R. Kijima, and T. Ojika, 1997, "Transition between virtual environment and workstation environment with projective head-mounted display", *Proc. of IEEE VR 1997*, Los Alamitos, CA, USA, 130-137, (1997)
4. J. Fergason, "Optical system for head mounted display using a retro-reflector and method of displaying an image," U.S. patent 5,621,572, April 15, 1997.
5. H. Hua, A. Girardot, C. Gao, J. P. Rolland, "Engineering of head-mounted projective displays". *Applied Optics*, 39 (22), pp.3814-3824, (2000)
6. H. Hua, C. Gao, F. Biocca, and J. P. Rolland, "An Ultra-light and Compact Design and Implementation of Head-Mounted Projective Displays", *Proc. of IEEE-VR 2001*, 175-182, (2001).
7. J. P. Rolland and Hong Hua, "Head-mounted displays," in *Encyclopedia of Optical Engineering*, R. Barry Johnson and Ronald G. Driggers, Eds, (2005).
8. C. Cruz-Neira, D. J. Sandin, and T. A. DeFanti, "Surround-screen projection-based virtual reality: the design and implementation of the CAVE", *Proc. of SIGGRAPH 1993*, ACM Press/ACM SIGGRAPH, New York, NY, USA. 135-142, (1993).
9. H. Hua, Y. Ha, and J. P. Rolland, "Design of an ultra-light and compact projection lens," *Applied Optics*, 42(1), 1-12, (2003).
10. Y. Ha, H. Hua, R. Martins and J. P. Rolland "Design of a wearable wide-angle projection color display" *Proceedings of SPIE* 4832, 67-73, (2002).
11. H. Hua, C. Gao, "A Polarized Head-Mounted Projective Display," *ACM International Symposium on Mixed and Augmented Reality*, 32- 35, (2005)
12. K. Daniel, "Speed May Give Ferroelectric LCOS Edge in Projection Race," *Display Devices Fall '05*
13. Teledyne Lighting & Display Products, <http://www.teledynelighting.com/>
14. M. Robinson, J. Chen, and G. Sharp, *Polarization Engineering for LCD Projection*. John Wiley & Sons, Ltd. England, 2005
15. M. C. Ruda, T. W. Stuhlinger., K. J. Garcia, "Solid state light engine optical system", US patent application 20050036119, Feb.17, 2005.
16. Fresnel Technologies, Inc., <http://www.fresneltech.com/>
17. Optical research Associates, <http://www.opticalres.com/>
18. H. Hua, C. Gao, and J. P. Rolland, "Study of the imaging properties of retro-reflective materials used in head-mounted projective displays," *Proceedings of SPIE (Aerosense 2002)*, Vol. 4711, pp.194-201 (2002)
19. N. Nanba, "Objective lens and image pickup device using the same", US patent 6,236,521, May 22, 2001.